Micro-PINGUIN: Microtiter plate-based ice nucleation detection in gallium with an infra-red camera

Corina Wieber[1,2], Kai Finster[1,3], Claus Melvad[4,5], Mads Rosenhøj Jeppesen[5], Tina Šantl-Temkiv[1,2,3,4]

[1]Department of Biology, Microbiology, Aarhus University, Aarhus, 8000, Denmark
[2]iCLIMATE Aarhus University Interdisciplinary Centre for Climate Change, Roskilde, 4000, Denmark
[3]Stellar Astrophysics Centre, Department of Physics and Astronomy, Aarhus University, Aarhus, 8000, Denmark
[4]Arctic Research Centre, Aarhus University, Aarhus, 8000, Denmark
[5]Department of Mechanical and Production Engineering, Aarhus University, Aarhus, 8000, Denmark

Correspondence to: Tina Šantl-Temkiv (temkiv@bio.au.dk)

Abstract.

Ice nucleation particles play a crucial role in atmospheric processes e.g., they can trigger ice formation in clouds and thus influence their lifetime and optical properties. The quantification and characterisation of these particles require reliable and precise measurement techniques. In this study, we present a novel droplet freezing instrument to measure immersion freezing of biotic and abiotic ice-nucleating particles within the temperature range of 0°C to -25°C. Immersion freezing of the samples is investigated using 384-well PCR plates with a sample volume of 30 µl. Nucleation events are detected with high precession using a thermal camera that records the increase in infra-red emission due to the latent heat release. To maximize the thermal contact between the PCR plate and the surrounding cooling unit we use a gallium bath as a mount for the PCR plate. The combination of good thermal connectivity and precise temperature recording enables accurate and reproducible detection of the nucleation temperatures.

For comparison with already existing instruments, the new ice nucleation instrument, "micro-PINGUIN", was characterized using Snomax® (hereafter Snomax) and Illite NX suspensions. The results are in agreements with what has been reported in the literature for the already existing set ups. Consequently, the results that will be produced using micro-PINGUIN are of similar quality as the results produced by other validated instruments for the study of immersion freezing of various ice nucleating particles. Further, we investigated the reproducibility of experiments using Snomax suspensions and found poor reproducibility when suspensions were prepared freshly even if the same batch of Snomax is used. This could be attributed to substrate heterogeneity, aging effects, and possible dilution errors. The reproducibility of the measurements is greatly improved for Snomax suspensions that are prepared in advance and stored frozen in aliquots. Thus, we suggest the use of suspensions frozen in aliquots for further reproducibility measurements and intercomparison studies.

1 Introduction

Clouds play an important role for the Earth's radiative balance and the climate. Cloud properties such as reflectivity and cloud lifetime are to a large extend determined by the properties of atmospheric aerosols. Precipitation from mixed-phase and cold clouds that is initiated via the formation of ice particles significantly contributes to the global water cycle (Mülmenstädt et al., 2015). While homogenous freezing of cloud droplets only takes place in cold clouds (< -37°C), ice nucleating particles (INPs) are required to initiate freezing in mixed-phase clouds (between 0°C and -37°C) (Murray et al., 2010). So far only biological INPs were shown to initiate ice formation at temperatures higher than -13°C at atmospherically relevant concentrations. This can result in a high fraction (up to 83% in the Arctic) of ice-containing clouds within this temperature range (Griesche et al., 2021).

To study the nature and concentration of INPs, a variety of droplet freezing techniques (DFTs) have been developed. These DFTs essentially differ in 1. the sample volume, 2. the number of droplets investigated per run, 3. the cooling system, 4. the method used for detection of nucleation events, 5. the temperature measurement. An overview of various DFTs is given in Miller et al. (2021). The volume used to investigate the ice nucleation efficiency in a sample has a big impact on the type of INPs that can be detected. Instruments with nanolitre and picolitre volumes are primarily used to investigate abundant INPs active at low temperatures (Peckhaus et al., 2016; Reicher et al., 2018; Chen et al., 2018; Budke and Koop, 2015). For these small volumes, the probability of contamination in the negative control is lower, which leads to low freezing temperatures of typically between -30°C to -37°C, thus activity can be investigated for samples that nucleate close to the temperatures at which homogenous freezing is initiated. However, low volume set-ups require a high concentration of INPs in the sample to be detected, thus making it less suitable for the analysis of high-temperature INPs, which are often present at low concentrations. In contrast, instruments with larger sample volumes, allow the study of rare INPs. However, with larger volumes the presence of impurities in the water control is becoming more likely, leading to a higher background freezing temperature. Consequently, it is challenging to study INPs that are active at low temperatures with large volume DFTs as the freezing curves at lower temperatures start to overlap with the curves of the pure water background. For instruments with a sample volume of 50 µl, freezing events in the negative control, are reported between -20 °C and -27°C (Schiebel, 2017; Harrison et al., 2018; Miller et al., 2021; Beall et al., 2017; Barry et al., 2021; David et al., 2019; Gute and Abbatt, 2020).

Another difference between the droplet freezing instruments is the way they determine the freezing of the samples. To detect the freezing events, several instruments use an optical camera combined with a temperature sensor to measure the freezing temperatures. As the temperature is measured only at positions where a temperature sensor is placed, gradients

in the system lead to a reduced accuracy of the detected freezing points. To minimize these gradients, a good thermal conductivity of the materials used between the cooling unit and the sample are of great importance. Further, the detection of the freezing temperatures with an optical camera is usually not based on the detection of the ice nucleation event but is instead based on the change in brightness of the sample during the process of the whole droplet freezing. Thus, the detection of the nucleation temperature based on changing optical properties is challenged by the fact that the total freezing time can take up to several minutes in particular at higher volumes and temperatures relevant for biogenic INPs. Thus, it is difficult to determine the exact starting point of ice nucleation using an optical camera. Harrison et al. (2018), for example, reported a freezing time of 100 seconds for a 50 µl droplet freezing at -12°C. The delay between the nucleation event and the freezing of the whole droplet can thus result in an error >1.5 °C at -12°C and larger errors at higher nucleation temperatures relevant for biogenic INP.

Despite the differences in the design of various DFTs, it is important that the produced results are comparable with each other. Therefore, there has been a series of intercomparison studies of various instruments using substances such as Snomax (Wex et al., 2015) and Illite NX (Hiranuma et al., 2015). Snomax is a commercially available substance and consist of freeze-dried cell material of the ice nucleation active bacterium *Pseudomonas syringae* with freezing temperatures as high as -2°C and Illite NX is a mineral that contains Illite, Kaolinite, Quartz, Carbonate and Feldspar active at lower temperatures. Both substances were found to be suitable for intercomparison studies when handled carefully (same batch, similar concentrations, and short storage times). However, Polen et al. (2016) highlighted the necessity of short storage times in case of Snomax powder as they showed that the ice nucleation ability of very active Snomax proteins decreases over time even when storage in the freezer.
In this study we present a new ice nucleation instrument for **p**late-based **i**ce **n**ucleation detection in **g**alli**u**m with an **in**fra-red camera (micro-PINGUIN). A high accuracy is achieved by combining good thermal contact of the sample and the surrounding cooling unit with the detection of freezing events by an infra-red camera. The working principle and the validation of micro-PINGUIN is described in the following sections. Further, we discuss challenges of using Snomax as a suspension for intercomparison studies and reproducibility measurements due to inhomogeneities in the substance and aging effects.

2 Description of the instrument

The micro-PINGUIN instrument is composed of three main parts: the cooling unit, the airflow system, and the camera tower with an infra-red camera for the detection of freezing events.

The cooling unit of the micro-PINGUIN instrument is built up in different layers and consists of Peltier elements, a vapor chamber and a gallium bath (Figure 1) to achieve good thermal conductivity, reduce horizontal gradients, and optimize the cooling capacity of the system. The temperature and cooling gradient are controlled by two PID regulated Peltier elements (QuickCool HighTech 270W). By applying voltage on the Peltier elements, a temperature difference is achieved between the two sides of the element. A water-cooling bath (Alpha cool chiller 2000, Eiszeit) is connected to the cooling unit and circulates precooled water (2°C) through the water cooler base plates (Plate Aqua Computer cuplex kryos NEXTsTRX4 Full Cover). Thereby the heat generated on the lower side of the Peltier elements is removed. The Peltier elements are immersed into a copper base and connected by thermal pads. Above the lower copper plate, a vapor chamber is used to distribute the cold evenly and thus to minimize horizontal temperature gradients within the system. A second copper base is positioned above the vapor chamber. It contains a fix-point cavity for the temperature measurement with the infrared camera and a thermistor probe (TE Connectivity 2.252 kΩ) at the same position to achieve precise temperature measurements as described in paragraph 2.3. The upper copper base contains a gallium bath that melts at around 30°C. A 384-well PCR plate that contains 30 µl of the sample volume per well can be submerged in the melted gallium bath that solidifies when cooled to room temperature. Thereby good thermal contact between the PCR plate that contains the samples and the cooling unit is obtained.

The freezing events and the temperature measurement are detected with a thermal camera (FLIR A655sc, Teledyne Flir) that is mounted in a black painted camera tower and positioned above the PCR plate. A continuous airflow of low relative humidity (<10% RH) is circulated within the camera tower to keep the humidity low and thus avoid condensation of water vapor on the PCR plate, which would interfere with the experiments. The instrument is controlled by a custom-made software (Ice Nucleation Controller). Per default, a cooling run is started at 10°C with a cooling rate of 1°C/min until the final temperature of -30°C is reached.

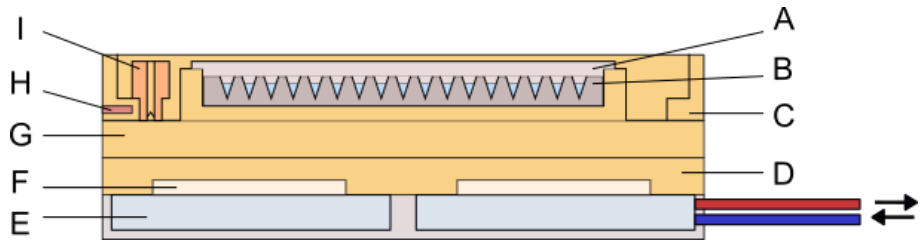

Figure 1: Schematic drawing of the cooling base. (A) 384-well PCR plate with the samples, (B) gallium bath, (C) top copper base, (D) bottom copper base, (E) water cooler base, (F) Peltier elements, (G) vapor chamber, (H) thermistor probe, (I) fix-point cavity for temperature calibration.

2.1 The role of the gallium bath

For an optimal cooling performance of the system materials with high thermal conductivity must be used. Aluminium is a commonly used material in PCR plate based systems (Schiebel, 2017; Kunert et al., 2018; Beall et al., 2017; Hill et al., 2014) as it has a good thermal conductivity and is fairly easy to shape which makes it suitable for the PCR plates mount. However, it cannot be avoided that a thin layer of air between the PCR plate and the aluminium plate forms and because of the good insolating properties of air, the thermal contact between the cooling system and the samples is thus hampered. To maximize thermal contact with the sample while minimizing the manufacturing process of the PCR mounting plate, we used gallium as a mount for the PCR plate. Gallium is a metal with a relatively low melting temperature (29.78°C) but high thermal conductivity (29.308–37.681 W/m K) (Prokhorenko et al., 2000). In the micro-PINGUIN system we use gallium to connect the 384-well PCR plates to the cooling system. By reversing the polarity on the Peltier elements, the system can be heated to 40°C, causing the gallium to melt. The PCR plate is then inserted into the liquid gallium and the system is cooled to 10°C. During this process, the gallium solidifies while a close contact to the PCR plate is created, and any access air is pushed out. To achieve a uniform contact for the whole plate, a clean weight is placed on top of the PCR plate during solidification of the gallium.

For future versions of this setup, we are planning to make small modifications, demonstrating that the use of gallium has further advantages. As heating can have an impact on the ice nucleation activity of the samples, the wells are usually filled with the suspension after the heating-melting cycle. However, this procedure can be an additional advantage of using gallium as a mount for the PCR plate. The use of gallium as a heat conductive medium allows to apply precise heat treatments to the samples by controlling the temperature of the gallium bath. Consequently, previously measured plates

could be remeasured after heating the gallium to the desired temperatures. Heat treatments are a commonly used method to differentiate between biogenic and inorganic INPs, assuming that biogenic INPs will decrease in the ice nucleation activity when heated to sufficiently high temperatures (an overview of studies using heat treatments is given in Daily et al. (2022)). The approach presented here could substitute traditional heating methods such as ovens or water baths for treating the samples. This would not only simplify the experimental process but also facilitate accurate and reproducible heat treatments for ice nucleation activity studies.

Further, when using gallium as a mount for the PCR plates the system is not limited to one type of PCR plates. Small modifications to the system allow the use of 96-well plates instead of 384-well plates, thus extending the range of sample volumes and thus INP concentrations that can be investigated.

2.2 The airflow system

During initial tests of the micro-PINGUIN system, freezing temperatures as high as -13°C were observed for the negative control. Similar freezing temperatures were found for MilliQ water, tap water and ultra-pure water for molecular work and were not affected by filtration of the water, indicating that these high freezing temperatures are not caused by impurities in the water. During the experiments, condensation of water vapor on the copper base and the PCR plate was observed. Tests with a flow of dry air passing through the camera tower showed that condensation was avoided during the experiment and that the freezing temperatures decreased with increasing air flow until T_{50} temperatures, corresponding to the temperature where 50% of the droplets are frozen, of around -25°C are reached (Figure 2). These background freezing temperatures are common for freezing experiments with volumes in the µl range. Other instruments using volumes of 50 µl (Schiebel, 2017; Harrison et al., 2018; Miller et al., 2021) reported comparable frozen fraction curves obtained by measurements of their negative controls. These airflow experiments indicate that at high humidity conditions, the freezing was caused by condensed water on the plates instead of INPs in the suspension. Thus, we decided to apply a flow of dry air that is supplied on the top part of the camera tower to lower the humidity in the micro-PINGUIN system. Before each run, the camera tower is flushed with a high flow of dry air (20 lpm). The flow is reduced to 10 lpm during the experiment to minimize the disturbance of the samples and the introduction of warm air. With this procedure the T_{50} temperatures of the negative control observed in the experiments are usually around -25°C. Also other droplet freezing techniques apply a dry air flow or N_2 flow to the system to avoid frost formation (Schiebel, 2017; Budke and Koop, 2015).

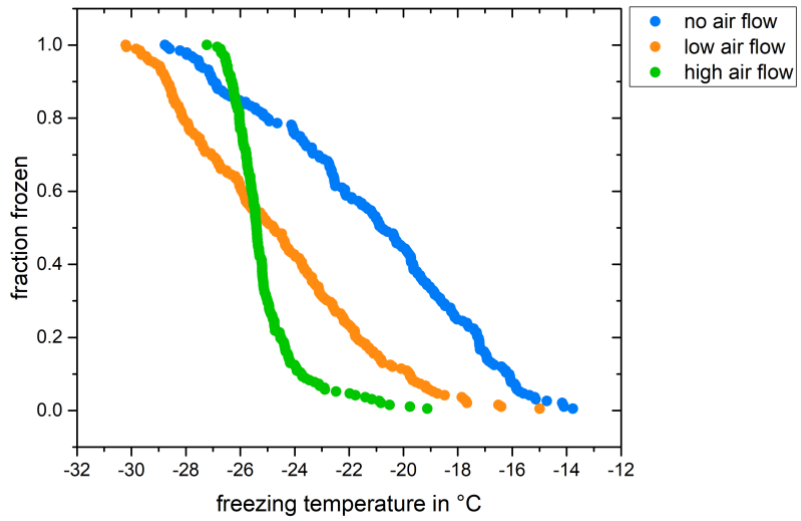

Figure 2: Effect of a dry air flow on the freezing behaviour of the negative control (MilliQ water). The high air flow corresponds to 20 lpm and the low flow to about 10 lpm. These freezing curves were obtained without flushing of the camera tower with dry air prior to the experiment.

2.3 Temperature measurement and detection of freezing events with a thermal camera

The temperature of the micro-PINGUIN instrument is measured with a thermal camera and a NTC thermistor in parallel. The thermal camera detects the infra-red radiation emitted by an object, in this case a microtiter plate well, and converts it into a visual image. As objects with a higher temperature emit more infra-red radiation than objects with a lower temperature and as the temperature is increasing during freezing due to latent heat, this technique can be used to measure the freezing temperatures of the samples. The camera is sensitive within a wavelength range of 7.5 to 14.0 µm and has a resolution of 640×480 pixels. It has a noise equivalent differential temperature (NEDT) of below 30 mK, which correlates to the minimum temperature difference that the camera can resolve. However, the thermal camera has a low absolute precision of ± 2°C, therefore a fix-point cavity is used as a reference measurement. The fix-point cavity is a copper tube with an angled bottom and a black inner surface. The radiation measured by the camera is scattered inside this cavity and gives a precise reading of the actual temperature T_{cavity}. The thermistor probe is positioned directly against the fix-point cavity and therefore measures the temperature $T_{\text{thermistor}}$ at the same position in the upper cooper base.

This temperature measurement is used as a reference temperature and its offset is applied to the temperature reading of the camera during the cooling experiment T_{camera}:

$$T_{\text{corrected}} = T_{\text{camera}} + (T_{\text{thermistor}} - T_{\text{cavity}}).$$

The thermistor has been calibrated with an AMETEK reference temperature calibrator (RTC-157) within a temperature range between +30°C to -35°C resulting in a final residual mean error of $\pm$ 15 mK. Further, the thermistor measurement serves as the input for the PID regulated Peltier elements during heating and cooling of the system.

During freezing of the sample, latent heat is released by the sample because of the phase change from water to ice. The initial phase of freezing when ice crystals start to form is a fast process resulting in an immediate temperature increase in the sample to 0°C. If this phase change is ongoing, the temperature stays at 0°C and a plateau forms. When the sample is completely frozen, no latent heat is released anymore, and the droplet cools down to ambient temperature. This results in a characteristic temperature profile for a freezing event as shown in Figure 3(b). The length of this plateau at 0°C is among other factors dependent on the temperature where the nucleation is initiated. For nucleation events close to 0°C, which is the case for some highly active biogenic INPs, the nucleation temperature and the temperature where the droplet is completely frozen can differ significantly. By using in infra-red camera for the detection of the freezing event we detect this immediate temperature increase upon nucleation as the freezing temperature of the sample. This is an advantage compared to the freezing point detection based on the change of the optical properties of the droplet. As long as the phase change is ongoing the optical properties of the droplets can change making it difficult to identify the exact moment of nucleation. Such variations in freezing point detection are especially crucial when investigating highly active INPs such as biogenic INPs.

Thus, in the micro-PINGUIN system a thermal camera captures an image of the PCR plate every 5 seconds and after each run, the data is processed by a custom-made software. This is done as follows: (1) A grid is created by the user, making sure that the location of every well is marked in the program (Figure 3a). (2) The temperature profile is then processed for each well and the freezing event is detected as a change in the slope of the temperature of each well (Figure 3b).

As the change in temperature is smaller for freezing events close to 0°C these temperatures can cause difficulties in the automatic recognition of the nucleation temperature. By default, a freezing event is recognized when the temperature gradient shows deviation in the temperature profile that is larger than two times the standard deviation.

This value can be lowered to identify nucleation events at high temperatures. To avoid false detections, the value with the largest deviation in temperature is always used as the freezing temperature.

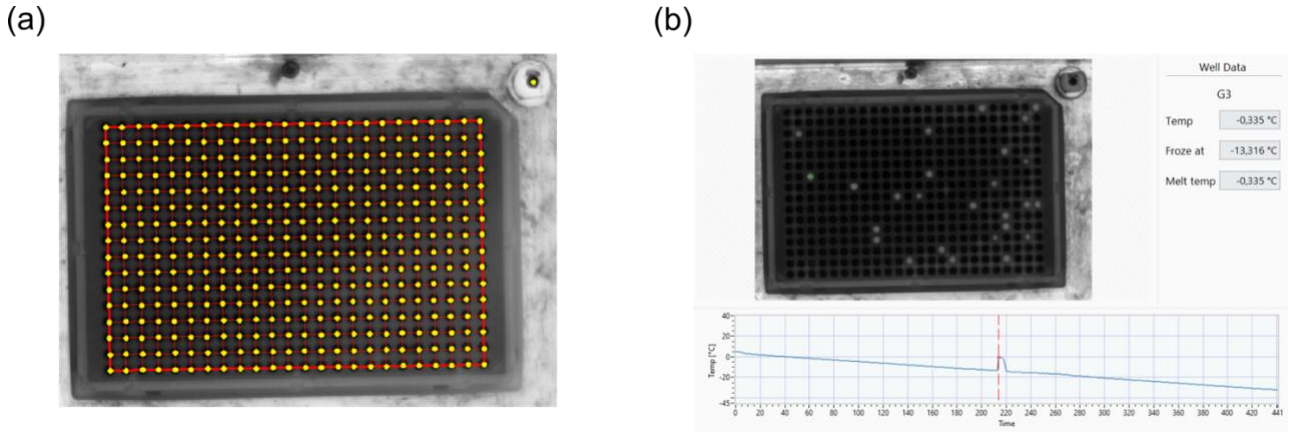

Figure 3: (a) Mask created for the freezing point detection. The yellow circles mark the pixels taken for the analysis. (b) Temperature profile of the droplet marked in green. The red line indicates the point in time with the highest temperature gradient.

2.4 Data analysis

Droplet freezing methods rely on splitting samples into multiple equal volumes and observing the freezing process of these volumes at varying temperatures (known as freezing curves) while maintaining a consistent cooling rate. However, it is important to note that droplet freezing assays have limitations in distinguishing solely between the liquid and frozen states of the droplets. Once the most potent INP among the mixture of INPs, initiates freezing and prompts droplet crystallization, the influence of less potent INPs becomes indistinguishable. To comprehensively investigate the freezing characteristics of highly reactive samples across a broad spectrum of temperatures, it is necessary to employ dilution series. Through this approach, the most potent INPs will be outdiluted, enabling the analysis of the INPs active at lower temperatures. Calculating the quantity of INPs based on the proportion of frozen droplets necessitates considering the particle concentration within the solution, the volume of the droplets, and the dilution factor.

Following the approach by Vali (1971) and assuming time independence of freezing, the cumulative spectrum K(T), corresponding to the number of sites active above temperature T per unit sample volume is described by

$$K(T) = -\frac{1}{V}\ln\left(1 - \frac{N_{\mathrm{f}}(T)}{N_0}\right), \tag{1}$$

with V the droplet volume, $N_f(T)$ the number of frozen droplets at a given temperature and N_0 the number of total droplets per sample. Based on this equation the number of ice nucleation active sites per mass of sample $n_m(T)$ is calculated as

$$n_{\mathrm{m}}(T) = -\frac{1}{V}\ln\left(1 - \frac{N_{\mathrm{f}}(T)}{N_0}\right)\left(\frac{d}{c_{\mathrm{m}}}\right),$$

using the dilution factor d and the particle mass concentration c_m.

3 Validation of the system

3.1 Snomax

The validation of the micro-PINGUIN instrument involved the use of extensively researched materials, and the obtained outcomes were juxtaposed with outcomes from established ice nucleation instruments. As part of the INUIT (Ice Nuclei research UnIT) initiative, comparative assessments of various ice nucleation instruments were conducted, employing Snomax (Wex et al., 2015) and Illite NX (Hiranuma et al., 2015). Snomax is commercially available and consist of freeze-dried cell material of the ice nucleation active bacterium *Pseudomonas syringae* and is ice nucleation active already at temperatures as high as -2°C (Wex et al., 2015). As the activity of Snomax decreases over time, for validation purpose a new batch was ordered from the manufacturer and stored at -20°C until usage. Care was taken that Snomax was not subjected to many temperature changes, as recommended by the manufacturer. To cover the temperature range of INPs that are active at lower temperatures, Illite NX powder was used. Illite NX powder consist of different minerals such as Illite, Kaolinite, Quartz, Carbonate and Feldspar. As the same batch of Illite NX is used as in the INUIT intercomparison study our results can be directly compared to the results reported by Hiranuma et al. (2015).

Measurements with Snomax suspensions of concentrations ranging from 10^{-2} mg ml^{-1} to 10^{-7} mg ml^{-1} were repeated three times and the average and standard deviation was calculated for the freezing curves. Results are showcased alongside the data acquired by Wex et al. (2015) in Figure 4(a). The measurements obtained with micro-PINGUIN show freezing of Snomax as high as -3.5°C. At -12°C, concentrations of INPs reach a plateau at 10^9 INPs per mg of Snomax. At the knee point around -10°C, INP concentrations obtained in this study are slightly below the values of previous measurements

with other instruments, but the plateau reached by the curve is in agreement with that reported by Wex et al. (2015). We noted significant discrepancies in repeated Snomax measurements, even when employing the identical instrument and the same batch of Snomax. As Snomax contains freeze-dried cells of *P.syringae* bacteria but also fragments of the cell membrane, remains of the culture medium and other unknown material, the number of INPs can vary within the prepared suspension leading to large variations in the measured freezing curves. Consequently, minor disparities in freezing spectra measured by diverse instruments are expected if different suspension are used. Furthermore, the variance in ice nucleation activity could potentially stem from the utilization of distinct batches of Snomax in the two studies, variations within the substrate or the possibility of marginal reduction in Snomax activity due to storage. We could significantly improve the reproducibility of the measurements by using aliquots of a Snomax suspension that was stored frozen until usage as shown in Figure 4(b). Thus, we propose the use of Snomax suspensions that are prepared in advance and stored frozen in aliquots for reproducibility measurements and further instrument intercomparison studies. The reproducibility of measurements using frozen aliquots is further discussed in paragraph 3.3.

3.2 Illite NX

The number of INPs normalized to the surface area $n_{s,BET}(T)$ measured for Illite NX suspensions of concentrations between 10 mg ml^{-1} and 0.1 mg ml^{-1} is shown in Figure 5 in comparison to data from other devices using Illite NX suspensions. $n_{s,BET}(T)$ was derived from the $n_m(T)$ spectrum following the approach by Hiranuma et al. (2015):

$$n_{\mathrm{s,BET}}(T) = \frac{n_{\mathrm{m}}(T)}{\theta},$$

with the specific surface area θ obtained from gas-adsorption measurements (BET-derived surface area) of 124.4 m^2 g^{-1}. We assume the same surface area as an aliquot sourced from the same batch of Illite NX as the one used by Hiranuma et al. (2015).

The data displayed in Figure 5 presents the mean and standard deviation derived from three measurements. The measurements conducted on Illite NX demonstrated commendable reproducibility. Freezing started at around -6.7°C with a concentration of 5.1×10^{-1} INPs per m^2 of Illite NX. The measurements obtained in this investigation fall in the lower end of the spectra recorded by other devices using a polydisperse Illite NX suspension (Hiranuma et al., 2015; Beall et al., 2017; Harrison et al., 2018), but are within the range of the concentrations reported therein. As a result, the measurements for both substances align favourably with data reported in earlier research, particularly when accounting for variations among various instruments.

(a)

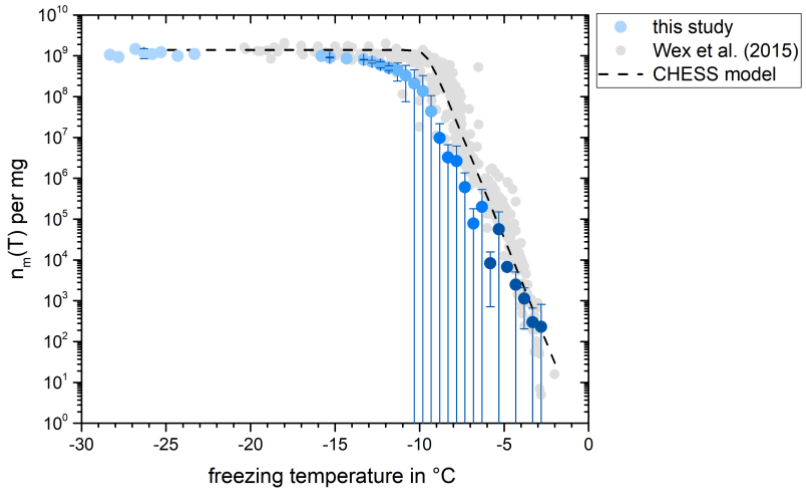

(b)

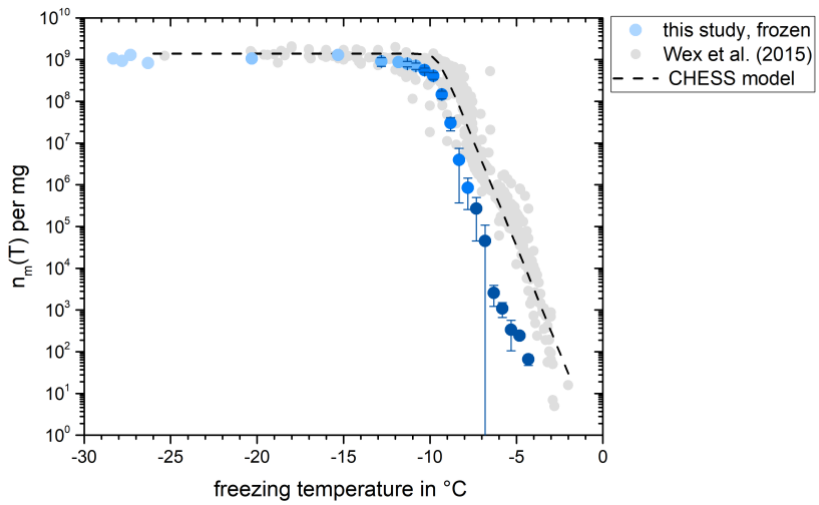

Figure 4: (a) Average number of INPs per mg Snomax measured for suspensions with 10^{-2} mg ml^{-1} to 10^{-7} mg ml^{-1} Snomax prepared freshly on three different days. The data was binned in 0.5°C temperature bins. Average and standard deviations are calculated for three experiments (blue data). Grey data points represent the results from various ice nucleation instruments investigated by Wex et al. (2015). The dashed line is based on the CHESS model by Hartmann et al. (2013). (b) The same is shown as in (a) but with the Snomax suspension that was prepared once, stored frozen in aliquots, and the measurement was repeated on freshly thawed aliquots three times.

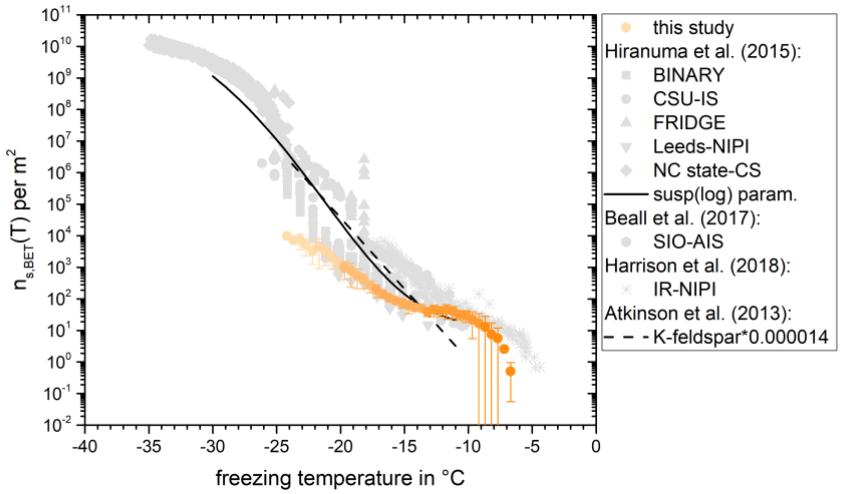

Figure 5: Average and standard deviations are calculated for three experiments of Illite NX (orange data). The grey data points represent measurements for comparable instruments (Hiranuma et al., 2015; Harrison et al., 2018; Beall et al., 2017). The black line shows the fit for all suspension measurement techniques in the logarithmic representation and the dashed line the fit from Atkinson et al. (2013) for K-feldspar multiplied with a factor of 0.000014 as discussed in Hiranuma et al. (2015).

3.3 Reproducibility of the measurements

To assess the consistency of measurements conducted with the micro-PINGUIN system, successive experiments were carried out employing the identical suspension. This approach aimed to mitigate the influence of dilution errors and variations within the substrates, enhancing the reliability of the results. Initial trials involving Snomax, Illite, and Feldspar suspensions revealed an aging phenomenon over the course of the day, despite storing the suspensions in the refrigerator between the individual experiments. As a result, the suspensions were freshly prepared immediately prior to each experiment, or the suspension was divided into portions that were frozen for preservation until needed. In the latter case, the samples were thawed just prior to conducting the ice nucleation experiment, and all measurements were executed within the same day to minimize disparities in freezer storage time. For characterizing this procedure, Snomax was chosen as the test substance due to its biogenic origin and the notable deviations in previous measurements. Figure 6 shows the mean value and standard deviation of the fraction frozen for three measurements with a concentration between 10^{-2} mg ml^{-1} and 10^{-7} mg ml^{-1} Snomax. The experiment's standard deviations range from 0.1°C to 0.35°C, showing outliers for exceedingly high and low INP counts respectively. Reproducibility within freezing temperatures ranging from -7°C to -10°C outperformed that at higher temperatures, likely due to the prevalence of Type C INPs over the

Type A which results in a higher Type C homogeneity. The mean standard deviation for this dataset is 0.2°C, leading to an estimated reproducibility of ±0.2°C for the micro-PINGUIN instrument. We suggest that this is a conservative estimate due to the difference in prevalence of Type A and Type C INPs in the sample. Thus, while the standard deviations observed for the temperature range, where Type A INP show predominant activity, are due to a combined effect of the technical reproducibility of our system and inhomogeneity of the INPs across the droplets, the standard deviations observed for the temperature range, where Type C INP show predominant activity, reflect primarily the technical reproducibility of our system.

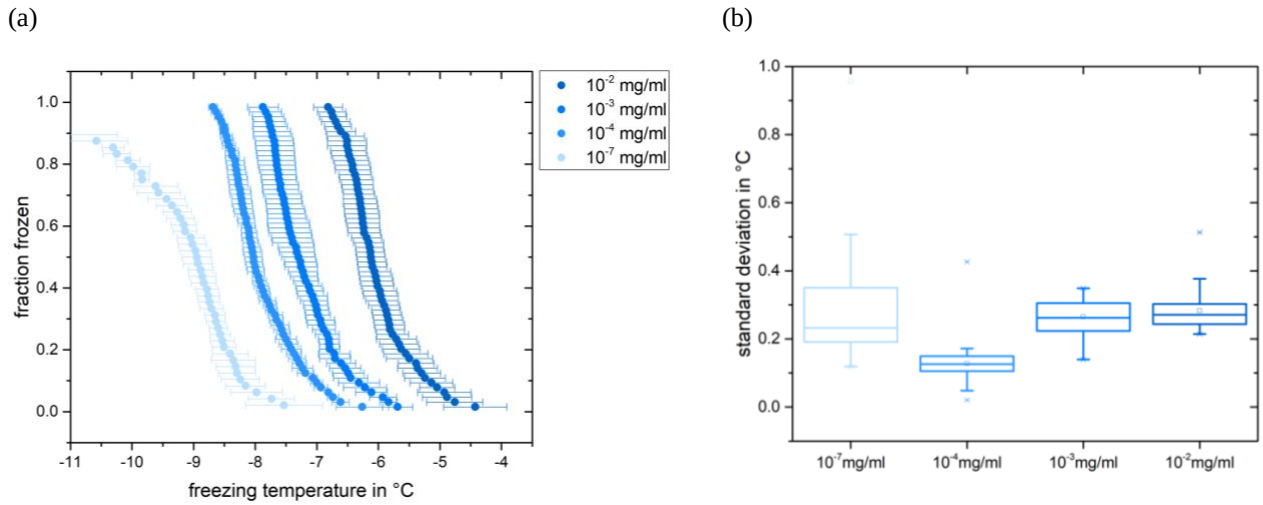

Figure 6: (a) Fraction frozen for Snomax suspensions with a concentration between 10^{-2} mg ml^{-1} and 10^{-7} mg ml^{-1}. The data for 10^{-5}mg ml^{-1} and 10^{-6} mg ml^{-1} are not shown for illustrative purposes. Data points represent the mean values of three measurements and their standard deviation. (b) Standard deviations for the different concentrations shown as box plots with 25th and 75th percentiles.

4 Conclusion

We developed a novel ice nucleation instrument that supports accurate nucleation temperature detection. The distinctive feature of this configuration is the utilization of a gallium bath, which acts as a platform that holds the PCR plates. The gallium bath ensures a good contact between the sample and the surrounding cooling unit. Further, the freezing events are detected with high precision by an infra-red camera based on a sudden rise in temperature following the nucleation event and facilitating recognition of nucleation events instead of freezing events, further reducing the error in assigned freezing temperatures. The micro-PINGUIN system was validated using the well-studied substances Snomax and Illite NX.

The results obtained in this study are consistent with already existing instruments. Based on the reproducibility experiments, we recommend that the Snomax suspensions are prepared in advance and stored frozen in aliquots for the future reproducibility and instrument intercomparison measurements.

Author contributions. All authors contributed to the development and design of micro-PINGUIN. The setup was manufactured by CM and MRJ. The experiments were conducted by CW. The analysis software was developed by MRJ. The paper was written by CW, with contributions from TST and KF. The project was supervised by TST and KF.

Competing interests. The authors declare that they have no conflict of interest.

Financial support. This work was supported by The Villum Foundation (23175 and 37435), The Carlsberg Foundation (CF21-0630), The Novo Nordisk Foundation (NNF19OC0056963), and The Danish National Research Foundation (DNRF106, to the Stellar Astrophysics Centre, Aarhus University).

5 References

Atkinson, J. D., Murray, B. J., Woodhouse, M. T., Whale, T. F., Baustian, K. J., Carslaw, K. S., Dobbie, S., O'Sullivan, D., and Malkin, T. L.: The importance of feldspar for ice nucleation by mineral dust in mixed-phase clouds, Nature, 498, 355-358, 10.1038/nature12278, 2013.

Barry, K. R., Hill, T. C. J., Jentzsch, C., Moffett, B. F., Stratmann, F., and DeMott, P. J.: Pragmatic protocols for working cleanly when measuring ice nucleating particles, Atmospheric Research, 250, 105419, https://doi.org/10.1016/j.atmosres.2020.105419, 2021.

Beall, C. M., Stokes, M. D., Hill, T. C., DeMott, P. J., DeWald, J. T., and Prather, K. A.: Automation and heat transfer characterization of immersion mode spectroscopy for analysis of ice nucleating particles, Atmos. Meas. Tech., 10, 2613-2626, 10.5194/amt-10-2613-2017, 2017.

Budke, C. and Koop, T.: BINARY: an optical freezing array for assessing temperature and time dependence of heterogeneous ice nucleation, Atmos. Meas. Tech., 8, 689-703, 10.5194/amt-8-689-2015, 2015.

Chen, J., Wu, Z., Augustin-Bauditz, S., Grawe, S., Hartmann, M., Pei, X., Liu, Z., Ji, D., and Wex, H.: Ice-nucleating particle concentrations unaffected by urban air pollution in Beijing, China, Atmos. Chem. Phys., 18, 3523-3539, 10.5194/acp-18-3523-2018, 2018.

Daily, M. I., Tarn, M. D., Whale, T. F., and Murray, B. J.: An evaluation of the heat test for the ice-nucleating ability of minerals and biological material, Atmos. Meas. Tech., 15, 2635-2665, 10.5194/amt-15-2635-2022, 2022.

David, R. O., Cascajo-Castresana, M., Brennan, K. P., Rösch, M., Els, N., Werz, J., Weichlinger, V., Boynton, L. S., Bogler, S., Borduas-Dedekind, N., Marcolli, C., and Kanji, Z. A.: Development of the DRoplet Ice Nuclei Counter Zurich (DRINCZ): validation and application to field-collected snow samples, Atmos. Meas. Tech., 12, 6865-6888, 10.5194/amt-12-6865-2019, 2019.

Griesche, H. J., Ohneiser, K., Seifert, P., Radenz, M., Engelmann, R., and Ansmann, A.: Contrasting ice formation in Arctic clouds: surface-coupled vs. surface-decoupled clouds, Atmos. Chem. Phys., 21, 10357-10374, 10.5194/acp-21-10357-2021, 2021.

Gute, E. and Abbatt, J. P. D.: Ice nucleating behavior of different tree pollen in the immersion mode, Atmospheric Environment, 231, 117488, https://doi.org/10.1016/j.atmosenv.2020.117488, 2020.

Harrison, A. D., Whale, T. F., Rutledge, R., Lamb, S., Tarn, M. D., Porter, G. C. E., Adams, M. P., McQuaid, J. B., Morris, G. J., and Murray, B. J.: An instrument for quantifying heterogeneous ice nucleation in multiwell plates using infrared emissions to detect freezing, Atmos. Meas. Tech., 11, 5629-5641, 10.5194/amt-11-5629-2018, 2018.

Hartmann, S., Augustin, S., Clauss, T., Wex, H., Šantl-Temkiv, T., Voigtländer, J., Niedermeier, D., and Stratmann, F.: Immersion freezing of ice nucleation active protein complexes, Atmos. Chem. Phys., 13, 5751-5766, 10.5194/acp-13-5751-2013, 2013.

Hill, T. C. J., Moffett, B. F., DeMott, P. J., Georgakopoulos, D. G., Stump, W. L., and Franc, G. D.: Measurement of Ice Nucleation-Active Bacteria on Plants and in Precipitation by Quantitative PCR, Appl Environ Microbiol, 80, 1256-1267, doi:10.1128/AEM.02967-13, 2014.

Hiranuma, N., Augustin-Bauditz, S., Bingemer, H., Budke, C., Curtius, J., Danielczok, A., Diehl, K., Dreischmeier, K., Ebert, M., Frank, F., Hoffmann, N., Kandler, K., Kiselev, A., Koop, T., Leisner, T., Möhler, O., Nillius, B., Peckhaus, A., Rose, D., Weinbruch, S., Wex, H., Boose, Y., DeMott, P. J., Hader, J. D., Hill, T. C. J., Kanji, Z. A., Kulkarni, G., Levin, E. J. T., McCluskey, C. S., Murakami, M., Murray, B. J., Niedermeier, D., Petters, M. D., O'Sullivan, D., Saito, A., Schill, G. P., Tajiri, T., Tolbert, M. A., Welti, A., Whale, T. F., Wright, T. P., and Yamashita, K.: A comprehensive laboratory study on the immersion freezing behavior of illite NX particles: a comparison of 17 ice nucleation measurement techniques, Atmos. Chem. Phys., 15, 2489-2518, 10.5194/acp-15-2489-2015, 2015.

Kunert, A. T., Lamneck, M., Helleis, F., Pöschl, U., Pöhlker, M. L., and Fröhlich-Nowoisky, J.: Twin-plate Ice Nucleation Assay (TINA) with infrared detection for high-throughput droplet freezing experiments with biological ice nuclei in laboratory and field samples, Atmos. Meas. Tech., 11, 6327-6337, 10.5194/amt-11-6327-2018, 2018.

Miller, A. J., Brennan, K. P., Mignani, C., Wieder, J., David, R. O., and Borduas-Dedekind, N.: Development of the drop Freezing Ice Nuclei Counter (FINC), intercomparison of droplet freezing techniques, and use of soluble lignin as an atmospheric ice nucleation standard, Atmos. Meas. Tech., 14, 3131-3151, 10.5194/amt-14-3131-2021, 2021.

Mülmenstädt, J., Sourdeval, O., Delanoë, J., and Quaas, J.: Frequency of occurrence of rain from liquid-, mixed-, and ice-phase clouds derived from A-Train satellite retrievals, Geophysical Research Letters, 42, 6502-6509, https://doi.org/10.1002/2015GL064604, 2015.
Murray, B. J., Broadley, S. L., Wilson, T. W., Bull, S. J., Wills, R. H., Christenson, H. K., and Murray, E. J.: Kinetics of the homogeneous freezing of water, Physical Chemistry Chemical Physics, 12, 10380-10387, 10.1039/C003297B, 2010.

Peckhaus, A., Kiselev, A., Hiron, T., Ebert, M., and Leisner, T.: A comparative study of K-rich and Na/Ca-rich feldspar ice-nucleating particles in a nanoliter droplet freezing assay, Atmos. Chem. Phys., 16, 11477-11496, 10.5194/acp-16-11477-2016, 2016.
Polen, M., Lawlis, E., and Sullivan, R. C.: The unstable ice nucleation properties of Snomax® bacterial particles, Journal of Geophysical Research: Atmospheres, 121, 11,666-611,678, https://doi.org/10.1002/2016JD025251, 2016.

Prokhorenko, V., Roshchupkin, V., Pokrasin, M., Prokhorenko, S., and Kotov, V.: Liquid Gallium: Potential Uses as a Heat-Transfer Agent, High Temperature, 38, 954-968, 10.1023/A:1004157827093, 2000.

Reicher, N., Segev, L., and Rudich, Y.: The WeIzmann Supercooled Droplets Observation on a Microarray (WISDOM) and application for ambient dust, Atmos. Meas. Tech., 11, 233-248, 10.5194/amt-11-233-2018, 2018.

Schiebel, T.: Ice Nucleation Activity of Soil Dust Aerosols, Ph.D. thesis, Karlsruher Institut für Technologie (KIT), 10.5445/ir/1000076327, 2017.

Vali, G.: Quantitative Evaluation of Experimental Results an the Heterogeneous Freezing Nucleation of Supercooled Liquids, Journal of Atmospheric Sciences, 28, 402-409, 10.1175/1520-0469(1971)028<0402:Qeoera>2.0.Co;2, 1971.

Wex, H., Augustin-Bauditz, S., Boose, Y., Budke, C., Curtius, J., Diehl, K., Dreyer, A., Frank, F., Hartmann, S., Hiranuma, N., Jantsch, E., Kanji, Z. A., Kiselev, A., Koop, T., Möhler, O., Niedermeier, D., Nillius, B., Rösch, M., Rose, D., Schmidt, C., Steinke, I., and Stratmann, F.: Intercomparing different devices for the investigation of ice nucleating particles using Snomax® as test substance, Atmos. Chem. Phys., 15, 1463-1485, 10.5194/acp-15-1463-2015, 2015.